Transcription Elongation Factor ELL2 Drives Ig Secretory-Specific mRNA Production and the Unfolded Protein Response

Kyung Soo Park,*[,1] Ian Bayles,*[,1] Alec Szlachta-McGinn,* Joshua Paul,* Julie Boiko,* Patricia Santos,* June Liu,* Zhou Wang,[†] Lisa Borghesi,* and Christine Milcarek*

Differentiation of B cells into Ab-secreting cells induces changes in gene transcription, IgH RNA processing, the unfolded protein response (UPR), and cell architecture. The transcription elongation factor eleven nineteen lysine-rich leukemia gene (ELL2) stimulates the processing of the secreted form of the IgH mRNA from the H chain gene. Mice (*mus musculus*) with the ELL2 gene floxed in either exon 1 or exon 3 were constructed and crossed to CD19-driven cre/CD19^{+}. The B cell–specific ELL2 conditional knockouts (cKOs; ell2$^{loxp/loxp}$ CD19$^{cre/+}$) exhibit curtailed humoral responses both in 4-hydroxy-3-nitrophenyl acetyl–Ficoll and in 4-hydroxy-3-nitrophenyl acetyl–keyhole limpet hemocyanin immunized animals; recall responses were also diminished. The number of immature and recirculating B cells in the bone marrow is increased in the cKOs, whereas plasma cells in spleen are reduced relative to control animals. There are fewer IgG1 Ab-producing cells in the bone marrow of cKOs. LPS ex vivo–stimulated B220^{lo}CD138^{+} cells from ELL2-deficient mouse spleens are 4-fold less abundant than from control splenic B cells; have a paucity of secreted IgH; and have distended, abnormal-appearing endoplasmic reticulum. IRE1α is efficiently phosphorylated, but the amounts of Ig κ, ATF6, BiP, Cyclin B2, OcaB (BOB1, Pou2af1), and XBP1 mRNAs, unspliced and spliced, are severely reduced in ELL2-deficient cells. ELL2 enhances the expression of BCMA (also known as Tnfrsf17), which is important for long-term survival. Transcription yields from the cyclin B2 and the canonical UPR promoter elements are upregulated by ELL2 cDNA. Thus, ELL2 is important for many aspects of Ab secretion, XBP1 expression, and the UPR. ***The Journal of Immunology*****, 2014, 193: 4663–4674.**

Activation of B cells by cognate Ag or polyclonal stimulators like LPS results in a large shift in RNA processing to the secretory-specific form of Ig H chain mRNA (1) and to a considerable upregulation of the unfolded protein response (UPR) to accommodate the massive quantity of IgH protein that results (2). This also causes major structural accommodations and altered endoplasmic reticulum (ER) cellular architecture. B cell expansion follows after LPS or Ag stimulation to initially create extrafollicular plasmablasts. B cells can also enter the follicles and form germinal centers where memory and plasma cells (PCs) can form (3). Long-lived PCs can reside in the bone marrow where they express a number of receptors for survival factors (4). Opposing suites of transcription factors either maintain the B cell program (e.g., Pax5, Bach2, Bcl6) or promote and facilitate differentiation to Ab secretion (e.g., IRF4, Blimp1, XBP1) (5). The mRNA for transcription elongation factor eleven nineteen lysine-rich leukemia gene (ELL2) was elevated when Blimp-1 and IRF4 were turned on (2, 6, 7); we showed that addition to B cells of exogenous cDNA for ELL2 stimulates alternative RNA processing, resulting in the use of the IgH secretory-specific poly(A) site and the skipping of weak alternative exons in IgH and test substrates (1). ELL2 drives the association of positive transcription elongation factor b (pTEFb) to RNA polymerase II (RNAPII), thereby stimulating phosphorylation of ser-2 on the C termini of the elongating polymerase near the start of the IgH locus (1, 8, 9). Thus, the binding of ELL2 with the highly phosphorylated C-terminal domain of RNAPII, polyadenylation factors, Dot1L (the histone H3K79 methylase), and with histone H3 K79me3 modifications are all seminal to the changes in RNA processing seen at the IgH locus. However, it was not known whether ELL2 is required for secretory IgH production in the animal and at what stage.

It was also not known whether the related members in the ELL family could substitute for ELL2. Three mammalian ELL genes encode proteins that are engaged in transcription elongation with pTEFb and RNAPII (10). ELL1 is ubiquitously expressed, whereas ELL3, found in stem cells (11) and in unstimulated B cells (12), is reduced upon LPS stimulation. ELL2, and not the other ELLs, was

*Department of Immunology, University of Pittsburgh, Pittsburgh, PA 15261; and [†]Department of Urology, University of Pittsburgh Cancer Institute, Shadyside Medical Center, Pittsburgh, PA 15232

[1]K.S.P. and I.B. contributed equally to this work.

Received for publication June 25, 2014. Accepted for publication August 20, 2014.

This work was supported by National Science Foundation Grant MCB-0842725 to C.M.; National Institutes of Health (NIH) Training Grant T32 CA082084 to K.S.P.; NIH shared resources Grant P30CA047904 to the University of Pittsburgh Cancer Institute; NIH Grants R01 AI079047 and R21 AI105846 to L.B.; and NIH Grants 9R01CA186780 and R37DK051193 to Z.W. and J.L.

Address correspondence and reprint requests to Dr. Christine Milcarek, Department of Immunology, University of Pittsburgh, School of Medicine, E1059 BST Office, E1000b BST Lab, Terrace and Lothrop Streets, Pittsburgh, PA 15261. E-mail: milcarek@pitt.edu

The online version of this article contains supplemental material.

Abbreviations used in this article: AP, alkaline phosphatase; cKO, conditional knockout; ELL2, eleven nineteen lysine-rich leukemia gene; ER, endoplasmic reticulum; ES, embryonic stem; KLH, keyhole limpet hemocyanin; NP, 4-hydroxy-3-nitrophenyl acetyl; PC, plasma cell; pTEFb, positive transcription elongation factor b; QPCR, quantitative PCR; RNAPII, RNA polymerase II; RT, room temperature; T3, transitional 3; UPR, unfolded protein response; UPRE, UPR element; wt, wild type.

found in the super-elongation complex associated with HIV-1 TAR and Tat with pTEFb (13). ELL2 is elevated in PC differentiation (1) and germinal center cells, and is highly expressed in all myeloma cells surveyed for survival along with IRF4 (6), making it unique among its related family members. We therefore reasoned that deleting ELL2 specifically in B cells could alter the production of the IgH secretory-specific mRNA after activation of those cells.

Two different ELL2 conditional knockout (cKO) mice were generated, one in exon 1 and one in exon 3; both models showed impaired PC differentiation in vivo and in vitro. The endogenous levels of serum Ig were decreased in the $CD19^{cre}$-driven conditional ELL2 knockout mice. These mice showed impaired responses to immunizations with 4-hydroxy-3-nitrophenyl acetyl (NP)-Ficoll, a T-independent Ag, or NP-keyhole limpet hemocyanin (KLH), a T-dependent Ag; Ag-specific Ig production was significantly reduced in the knockouts relative to wild type (wt) mice. Recall responses were also affected. The splenic transitional 3 (T3) cells and PCs were significantly reduced in the cKOs, whereas bone marrow recirculating B cells were significantly increased in the knockouts. But IgG1-producing bone marrow cells were decreased in the knockout. Studies reported in this article with spleen cells from the $CD19^{cre}$ cKOs of ELL2 in B cells show that after LPS stimulation of resting B cells, the processing of IgH mRNA to the secretory-specific form was severely reduced, even in the small number of sorted $CD138^{+}B220^{lo}$ so-called PCs produced. The amount of the Ig chaperones and activators in the UPR was diminished, most especially ATF6, BiP, cyclin B2, and XBP1; Ig κ L chain and BCMA were also impaired in the knockouts. Thus, ELL2 is a key player not only in IgH mRNA processing, but also in subsequent Ab-secreting cell differentiation, making it exceptional in the ELL family of factors and crucial for PC development.

Materials and Methods

Generation of cKO mice

ELL2 is a single gene that resides on mouse chromosome 13. In collaboration with genOway (http://www.genoway.com), ~1 kb upstream of the transcription start site and aa 1–50 of exon 1 were surrounded by loxP sites in a conditional targeting vector (Fig. 1A), the vector was inserted into the genome in embryonic stem (ES) cells (129Sv/pas) and insertion of the construct selected for the neomycin marker in the targeting vector; the neo cassette was flanked by frt sites (see Supplemental Fig. 1 for the Southern blots showing proper integration into the ELL2 gene). The insertion and subsequent deletion was also detected by PCR (Fig. 1). After germline transmission of the targeted allele was established, the frt flanked neo cassette was removed by crossing to mice expressing *Flpe*. The mice were made homozygous for the exon1 loxp/loxp locus, then crossed to $CD19^{cre/+}$ mice ($Cd19^{tm1(cre)Cgn}$ Igh^{b}/J #006785, C57BL/6; Jackson Laboratories) to produce progeny that were ELL2 exon1 loxp/loxp $CD19^{cre/+}$. The $CD19^{cre}$ was chosen because it is B cell specific, is expressed throughout B cell development, maps to chromosome 7, and was previously used to elucidate the action of many other genes. The loxp-to-loxp distance after deletion is ~1.5 kb, and there is an XmaI site just upstream of the frt cassette. The deletion was detected using primers (CM 82437293 and 82437294) just beyond the loxp sites, as shown in Fig. 1: 11856cre-MICI 5′-AAGAGGATTGCTGTAGGCACCCTCC-3′ and 11857cre-MICI 5′-TCCCAGAAAACTCTGACCGCTCG-3′.

The wt allele produces a PCR band of 1806 bp, insertion of loxp produces a band of 1983 bp, whereas after cre-mediated excision the band is reduced to ~0.6 kb (see Fig. 1). The PCR conditions were 10 ng genomic DNA with 5% DMSO in reaction, denature 94°C 120 s, 1 cycle, then 35 cycles of denature 94°C 30 s, anneal 65°C 30 s, extend 68°C 300 s, and 1 cycle of Completion 68°C 480 s.

The ELL2 cKO mouse with the deletion of exon 3 (encoding aa 66–97) was cloned by June Liu from Dr. Zhou Wang's laboratory. We used ES cells (129Sv/pas), and insertion of the construct was selected for the neomycin marker in the targeting vector; the neo cassette was flanked by frt sites as described earlier for ELL2 exon 1 and shown in Supplemental Figs. 1 and 2. The insertion of the targeting vector was detected using Southern blotting and increased size of the EcoRI fragment on the 3′ side and insertion of a new SacI site on the 5′ side (Supplemental Figs. 1, 2). Genotyping the ELL2 mice from the Wang laboratory was conducted using PCR with ELL2ckoC(90446583) 5′-AGG AGT TCA AGG TCT GCA TC-3′ and ELL2ckoF(90446584) 5′-GGT GGA AAT CAC TCC TGT TC-3′.

The wt allele produces a PCR band of 400 bp, and insertion of loxp produces a band of 500 bp, as shown in Fig. 1C. When exon 3 is deleted, the 500-nt band disappears. GAPDH was used as control for DNA content. The PCR conditions were 10 ng genomic DNA, denature 94°C 120 s, 1 cycle, then 35 cycles of denature 94°C 30 s, anneal 55°C 30 s, extend 72°C 40 s, 1 cycle of Completion 72°C 300 s.

For genomic GAPDH, the primer sequences were as follows: GAPDH-F (13947763) 5′-GAG ACA GCC GCA TCT TCT TGT-3′ and GAPDH-R (13947764) 5′-CAC ACC GAC CTT CAC CAT TTT-3′. The PCR condition is the same as in the genotyping of ELL2, and the expected PCR band size is 75 bp.

To genotype $CD19^{cre/+}$ mice, we used primers for CD19 flanking the potential cre insertion site: CD19creF(50312489), 5′-GCG GTC TGG CAG TAA AAA CTA TC-3′; CD19creR(50312490): 5′-GTG AAA CAG CAT TGC TGT CAC TT-3′; CD19wtF(50312491), 5′-CCT CTC CCT GTC TCC TTC CT-3′; and CD19wtR(50312492), 5′-TGG TCT GAG ACA TTG ACA ATC A-3′.

CD19 wt gene produces a fragment of ~477 bp, whereas the CD19 cre shows a fragment of 100 bp. Heterozygotes show both bands. The PCR condition is the same as in the genotyping of ELL2. Isolation of genomic DNA was done using whole-blood samples collected from tail-vein bleeds using DNeasy Blood and Tissue Kit (69504; Qiagen) according to the manufacturer's instructions.

All mice were maintained at the University of Pittsburgh animal facilities, and experiments were undertaken and conducted in accordance with institutional policies, as per Animal Welfare Assurance number A3187-01.

Flow cytometry

Bone marrow and spleen were harvested from mice and processed as previously described (14, 15). Cell staining was performed using Abs to murine surface markers obtained from eBioscience or BD Pharmingen. Primary anti-mouse Abs were B220 (clone RA3–6B2), CD19 (clone MB19–1), CD43-PE (clone S7), AA4.1 (clone AA4.1), IgM (clone 331), IgD (clone 11-26), CD138 (clone 281-2), CD21 (clone eBioD9), CD23 (clone B3B4), CD5 (clone 53-7.3). Secondary reagents were streptavidin-Cy7PE or streptavidin-eFluor 450. Dead cells were excluded using DAPI. Flow cytometry was performed on a 4-laser, 12-detector LSR II or a 4-laser, 13-detector LSR Fortessa (BD Biosciences). Data were analyzed using FlowJo software. The schemes were derived from Santos et al. (16) and Winkelmann et al. (17), and are described more fully in Supplemental Table 1.

To sort cells for Ab-secreting PCs, we incubated LPS-induced splenocytes with allophycocyanin-conjugated Anti-Human/Mouse CD45R (B220; #47-0452; eBioscience) and PE-conjugated Rat Anti-Mouse CD138 (#553714; BD Biosciences) for 30 min on ice in the dark. Dead cells were excluded by DAPI staining. BCMA staining was done using Monoclonal Anti-mouse BCMA-Fluorescein (#FAB593F; R&D Systems).

ELISA

Assays were performed following standard procedures using Clonotyping System-AP (Southern Biotech, Birmingham, AL) on the 96-well plates (Dynex Immulux HB, Chantilly, VA). The kit with IgG2c antisera is necessary for the C57B/L6 mice that lack IgG2a (18). The plate was coated with 100 μl/well capture Ab (Goat anti-mouse Ig(H+L) to a concentration of 5 μg/ml in 1× PBS, pH 7.4. After overnight incubation at 4°C, the wells were treated with 10% BSA for 3 h at room temperature. Mouse serum was diluted 5000 times for IgG1 or 1000 times for other Ig isotypes and incubated with the plates overnight at 4°C. The wells were washed and alkaline phosphatase (AP)–labeled detection Abs (diluted 5000 times) were added and incubated for 1 h at room temperature. The wells were washed and developed using 1 mg/ml AP Substrate solution (Thermo Scientific, Waltham, MA) containing p-nitrophenyl phosphate for ≥15 min. The plate was read at A450. Standards were run for the various isotypes. For NP-specific Ig detection, plates were coated with NP-BSA (Biosearch Technologies, Petaluma, CA).

Immunizations

Six- to 8-wk-old ELL2 cKO mice and littermate control mice were immunized i.p. with either NP-Ficoll (F1420; Biosearch Technologies) at 25 μg in 0.1 ml PBS or 100 μg NP-KLH (N-5060; Biosearch Technologies) precipitated with alum (77161; Pierce) as previously described for blimp knockouts (19). Serum was collected at 1, 2, and 3 wk postinjection using NP-BSA–coated plates in an ELISA. For the recall response, the same dose

of NP-KLH was given 6 wk after the initial dose, and serum was collected at 7 and 14 d.

Western blot

Protein samples were obtained from nuclear and cytoplasmic extracts of 0 d and 3 or 4 d after LPS exposure using NE-PER Nuclear and Cytoplasmic Extraction Reagents (#78833; Thermo Scientific) according to the manufacturer's instructions. Protein samples were then measured for concentration by Bradford Assay. Western protocol followed was the Bio-Rad General Protocol for Western blotting (Bio-Rad Bulletin 6376 Rev A). m.w. markers used in the gels were the Precision Plus Protein Kaleidoscope markers from Bio-Rad (#161-0375). Before running protein samples on 10% Acrylamide Mini-PROTEAN TGX precast Gels (Bio-Rad Laboratories #456-1034), samples were boiled at 95˚C for 5 min and centrifuged at 16,000 × *g* in a microcentrifuge for 1 min. Samples were then loaded onto gels and run for 5 min at 50 V. The voltage was then increased to 165 V for ~1 h. After gels had run to desired length, the gel was placed in a 1× transfer buffer (25 mM Tris, 190 mM glycine 20% methanol, 1% SDS) for 15 min. After transfer to polyvinyldifluoride membrane, samples were analyzed by immunoblot and visualized by ECL using Pierce ECL Western blotting Substrate (#32209; Thermo Scientific). Blots were imaged on a ProteinSimple FluorChem M System.

Abs used

Primary Abs. Primary Abs used included XBP1 (M-186; sc-7160; Santa Cruz Biotechnology) m.w. 29/40 kDa; pAb anti-IRE1α [p Ser 724] Ab (NB100-2323; Novus Biologicals) m.w. 110 kDa; Rb pAb to IRE1 (ab37073; Abcam); ELL2 R4502 affinity-purified rabbit Ab (1); ATF-6α (H-280; sc-22799; Santa Cruz Biotechnology) m.w. 75–85 kDa; BIP (C50B12; 3177S; Cell Signaling Technology) m.w. 75 kDa; Anti-Mouse IgM (μ-chain–specific) Ab produced in goat (M8644-1MG; Sigma) m.w. >55kDa; Anti-Hu/Mo Blimp1 purified clone: 6D3 (14-5963-82; eBioscience) m.w. 110 and 150 kDa with sumoylation; IgM κ-chain m.w. 25 kDa; Cyclin B2 (H-105; sc-22776; Santa Cruz Biotechnology) m.w. 43kDa; YY1 (H-414; sc-1703; Santa Cruz Biotechnology); Monoclonal Mouse Anti-Actin Clone C4 (691001; MP Biologicals) m.w. 43 kDa.

Secondary Abs. Secondary Abs used included goat anti-rabbit IgG-HRP (sc-2004; Santa Cruz Biotechnology); donkey anti-goat IgG-HRP (sc-2020; Santa Cruz Biotechnology); goat anti-mouse IgG-HRP (sc-2005; Santa Cruz Biotechnology); and goat anti-rat IgG-HRP (sc-2006; Santa Cruz Biotechnology).

ELISPOT

Millipore MultiScreen 96-well Filter Plates (#MSIPS4W10; Millipore) were coated with 5–6 μg/ml goat anti-mouse H and L chain, purified Igs (#5300-04; Southern Biotech) for 2 h at room temperature (RT). Wells were then washed and blocked with cell media + 10% FCS for 1.5 h at RT. Live cells (sorted with DAPI), after 72 h post LPS exposure (20 μg/ml), were then added to the wells and allowed to incubate overnight at 37˚C. After incubation with Goat anti-mouse IgM-AP Abs (#5300-04; Southern Biotech) for 1.5 h at RT, spots were visualized with 1-Step NBT/BCIP solution (#34042; Thermo Scientific). Counting and imaging of spots was done on an Immunospot S6 Micro Analyzer using Immunspot 5.0 Professional software. For bone marrow samples, anti–IgG1-AP Ab was used.

B cell cultures

Splenocytes were extracted from mice and naive B cells selected by autoMACS using a B cell Isolation Kit (#130-090-862; Miltenyi Biotec) using a mixture of biotin-conjugated Abs against CD43 (Ly-48), CD4 (L3T4), and Ter-119, as well as Anti-Biotin MicroBeads. The splenocytes were counted by hemocytometer and cultured at a density of 1–5 × 10^6 cells/ml. Cells were cultured for 72 or 96 h with LPS at 20 μg/ml (LPS from *Escherichia coli* 00111:B4; #L3012-10MG; Sigma) in RPMI 1640 media with 50 μM 2-ME, 2 mM glutamine, 10% FCS, sodium pyruvate, nonessential amino acids, Pen/Strep, and HEPES buffer. A cell density of ~5 × 10^6 cells/ml was maintained by dilution in medium with LPS.

RNA isolation and RT-QPCR

NucleoSpin RNA II kits (740955.50; Clontech) were used to isolate RNA from cells at 0 and 72/96 h after LPS exposure. To create cDNA SuperScript First-Strand (11904-018; Invitrogen), kits were used according to manufacturer's instructions and dT primers. cDNA was then used in RT-quantitative PCRs (QPCRs) using SYBR Green PCR Master Mix (4309155; Applied Biosystems) reagents. Primers used for RT-QPCR are listed in Supplemental Table 2.

Luciferase

The mouse cyclin B2 promoter (-1188) cloned into the firefly luciferase pGL4.10 vector at the Kpn1 and Nco1 sites was a generous gift of Dr. Kurt Engeland, Universitatt Leipzig, Germany. This is similar to the previous cyclin constructs in which the inhibitory effect of p53 was demonstrated on the cyclin B2 promoter (20, 21). We cloned portions of the human blimp-1 (-2973 to 0), ELL2 (-3000 to 0), and IRF4 (-2182 to 0) promoters into pGL4.11 (Promega, Madison, WI). The expression cDNA plasmids for blimp-1 (CM#:632), c-Myc (CM#:633), ELL2 [CM#:56 7 (1)], IRF4 (CM#:594), p53 wt (CM#:634), mutant p53R175H (CM#:635), and the p65 subunit of NF-κB (Dr. Gutian Xiao, University of Pittsburgh Cancer Institute) were transfected in 12-well plates (Falcon, Franklin Lakes, NJ) with the indicated reporters in 293T cells using GenJuice (Novagen, San Diego, CA) as the transfection reagent. After 2 d, cells were lysed with 100 μl/well of 1× Reporter Lysis Buffer (Promega, Madison, WI), and luciferase activity was assayed with 20 μl of each lysate using the dual Luciferase Assay System (Promega) with a luminometer. The SR proteins were cloned into the mammalian expression plasmids pEF4his (Invitrogen). The original cDNAs were a generous gift of Martha Peterson (22) and Gavin Screaton (23). For each transfection, 200 ng of the firefly luciferase reporter plasmid 0.6 ng Renilla luciferase reporter (pRL-TK; Promega) was used as a control. Firefly luciferase values were normalized to the Renilla plasmid activity values.

Statistics

All experiments reported in this article were performed with samples from at least three different mice of the indicated genotypes or three different cell transfections. The results were plotted and analyzed using GraphPad PRISM 5; $*p = 0.05$, $**p = 0.01$, and $***p = 0.001$ are indicated on graphs. The *p* value was determined by either a two-tailed Student *t* test when two samples were analyzed, or in the case of multiple samples, using ANOVA with Tukey's or Bonferonni's posttests. Error bars represent SEM.

Results

cKO of ELL2 in B cells

Mice deficient in ELL1 (also known as MEN1) are embryonic lethal (24). To avoid the lethality that might accompany a complete loss of ELL2 in mice, we deleted ELL2 specifically in B cells. The strategy we used to make and detect deletions is drawn in Fig. 1A and described more completely in *Materials and Methods*, whereas the Southern blots showing proper integration are shown in Supplemental Figure 1. We independently targeted exon 1 in one strain of mice and exon 3 in another, because we were initially concerned that the loxp insertion in the ELL2 promoter region might compromise normal ELL2 expression elsewhere. Mice bearing the ELL2 exon1 loxP/loxP or exon3 loxP/loxP genes, diagramed in Fig. 1A, were crossed with mice carrying one copy of the cre recombinase coding sequence, driven by the B cell–specific CD19 promoter designated $CD19^{cre/+}$ (25). As illustrated in Fig. 1B, the deletion that occurs in splenic B cells of exon 1 in the ELL2 cKO, generating the shorter 0.6-kb PCR product, is >90%. The ELL2 exon3 loxp/loxp is also deleted in splenic B cells of mice carrying that insert (see Fig. 1C). In this assay, the specific PCR product encompassing the 5′ loxp site is virtually absent in the ELL2 exon 3 floxed splenic B cells, with the PCR product corresponding to the GAPDH gene serving as a positive loading control (see a later figure for a more complete deletion). To assess ELL2 protein expression in the cKO mice ($ELL2^{loxp/loxp}$ $CD19^{cre/+}$), we purified and stimulated $B220^+$ resting splenocytes with LPS for 3 or 4 d, a treatment that normally induces B cell proliferation and PC differentiation. When compared with control ($ELL2^{+/+}$ $CD19^{cre/+}$ or $ELL2^{loxp/loxp}$ $CD19^{+/+}$) splenocytes treated the same way, there was very little or no ELL2 protein expression in the cKO mice (Fig. 1D). The RNA from splenic B cells was isolated with and without 4 d of LPS exposure. The level of HPRT mRNA (set as 100%) was used as an internal RT-PCR control. As shown in Fig. 1E, the mRNA for ELL2 increases >6-fold relative to no LPS in the control mouse spleens, achieving levels greater than HPRT mRNA,

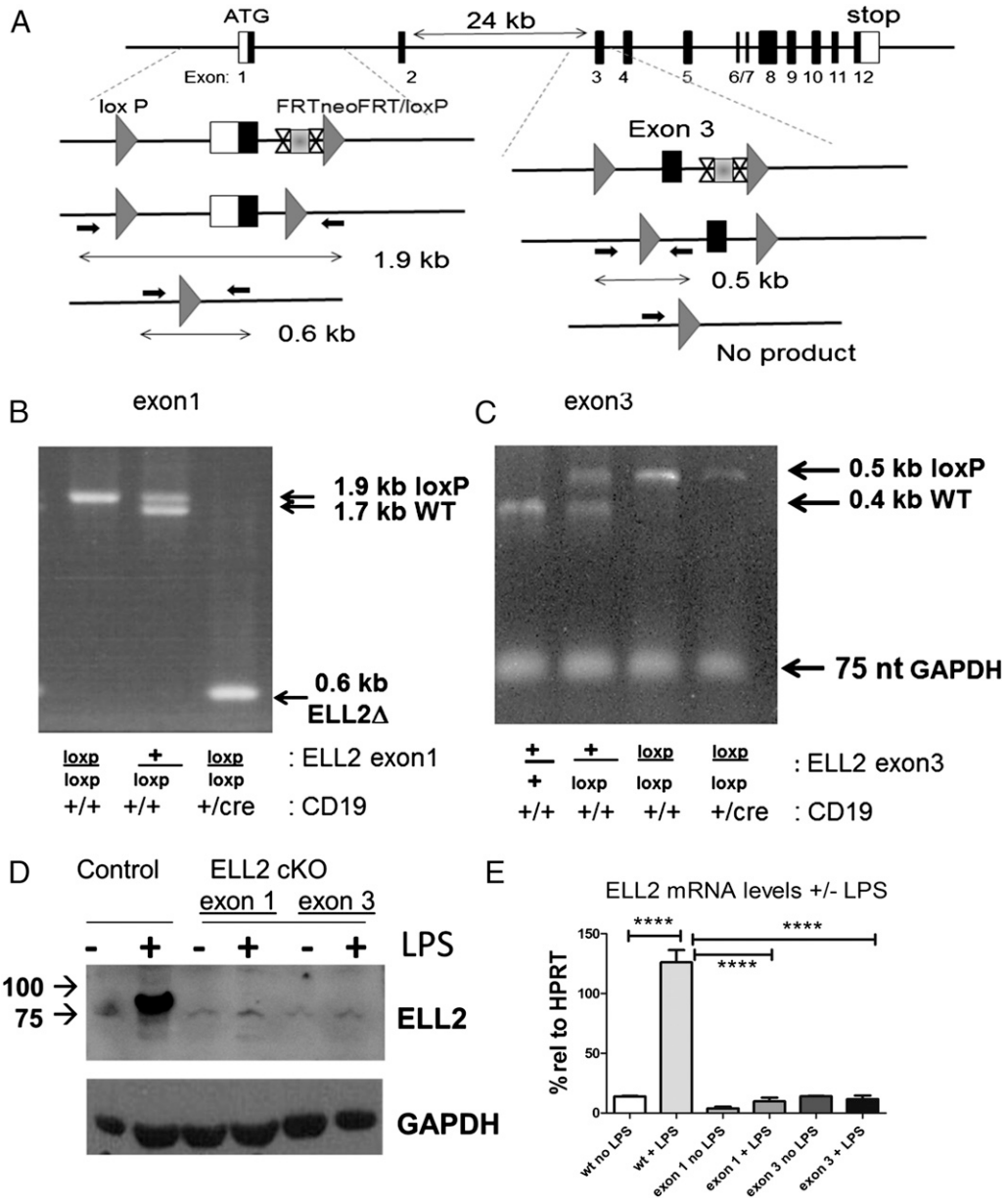

FIGURE 1. ELL2$^{loxp/loxp}$ mice have efficient deletion of ELL2 in B cells. (**A**) Strategy for generating alleles of ELL2 with either exon 1 or exon 3 flanked by loxp sites (triangles). The FRTneo gene flanked by sites indicated as X…X is deleted in ES cells in both models. Loxp sites are indicated by the gray triangles. Small arrows indicate the primers used to generate PCR fragments of 1.9 (plus two loxP sites) and 1.7 kb (no loxP) for exon 1. Deletion between the two loxP sites in the presence of CR19$^{cre/+}$ generates a 0.6-kb PCR fragment. Small arrows in exon 3 flank one of the loxP sites to generate PCR fragments of 0.5 (plus loxP) and 0.4 kb (no loxP). Absence of a 0.5-kb product indicates deletion between the two loxP sites with CD19$^{cre/+}$. (**B**) PCR analysis to detect the 0.6-kb deletion product in the presence of CD19$^{cre/+}$ in B cells. (**C**) PCR analysis showing deletion of the 0.5-kb fragment in the presence of CD19$^{cre/+}$. The GAPDH DNA PCR product indicates that there is the same amount of DNA in each sample. (**D**) Immunoblot of nuclear lysates from splenocytes ±20 μg/ml LPS for 4 d of ELL2$^{loxp/loxp}$ mice with CD19$^{cre/+}$ or CD19$^{+/+}$. Proteins were run on a denaturing polyacrylamide gel, blotted, and probed with affinity-purified rabbit anti-ELL2 peptide (R4502) as previously described. (**E**) mRNA levels of ELL2 with or without LPS stimulation 4 d after addition in control and ELL2$^{loxp/loxp}$ CD19$^{cre/+}$ mice was quantified relative to HPRT control RNA, set as 100% by real-time QPCR. $n > 5$ each group. Error bars indicate SEM. ****$p = 0.001$.

a housekeeping gene that is consistently expressed throughout B cell differentiation (26). The mRNA for ELL2 does not increase after LPS in either the ELL2 exon 1 or the exon 3 targeted mice, consistent with the gene deletion and protein results. Thus, the cre/loxp strategy is effective at eliminating ELL2 expression in these late stages of B cell development.

Reduction in Ig secretion in ELL2$^{loxp/loxp}$ CD19$^{cre/+}$ mice

To determine whether ELL2 has an effect on Ig secretion in the animal, we then conducted ELISA assays for the amount of secreted Ig in the serum of unimmunized control ELL2$^{loxp/loxp}$ CD19$^{+/+}$ or ELL2$^{+/+}$ CD19$^{cre/+}$ mice (combined data labeled wt on graphs) and the ELL2$^{loxp/loxp}$ CD19$^{cre/+}$ mice (cKO). We saw a decrease in the ELL2 exon 1 cKOs in serum levels of secreted IgM, IgG1, and IgA isotypes as shown in Fig. 2 and for all the other IgG isotypes (data not shown). With the ELL2 exon 3 cKO mice, the Ig levels were decreased ≥2-fold for IgM, IgG1, and IgA (Fig. 2), as well as for the other IgG isotypes (data not shown). ELL2 expression on stimulated B cells is thus required for Ig secretion in the whole animal.

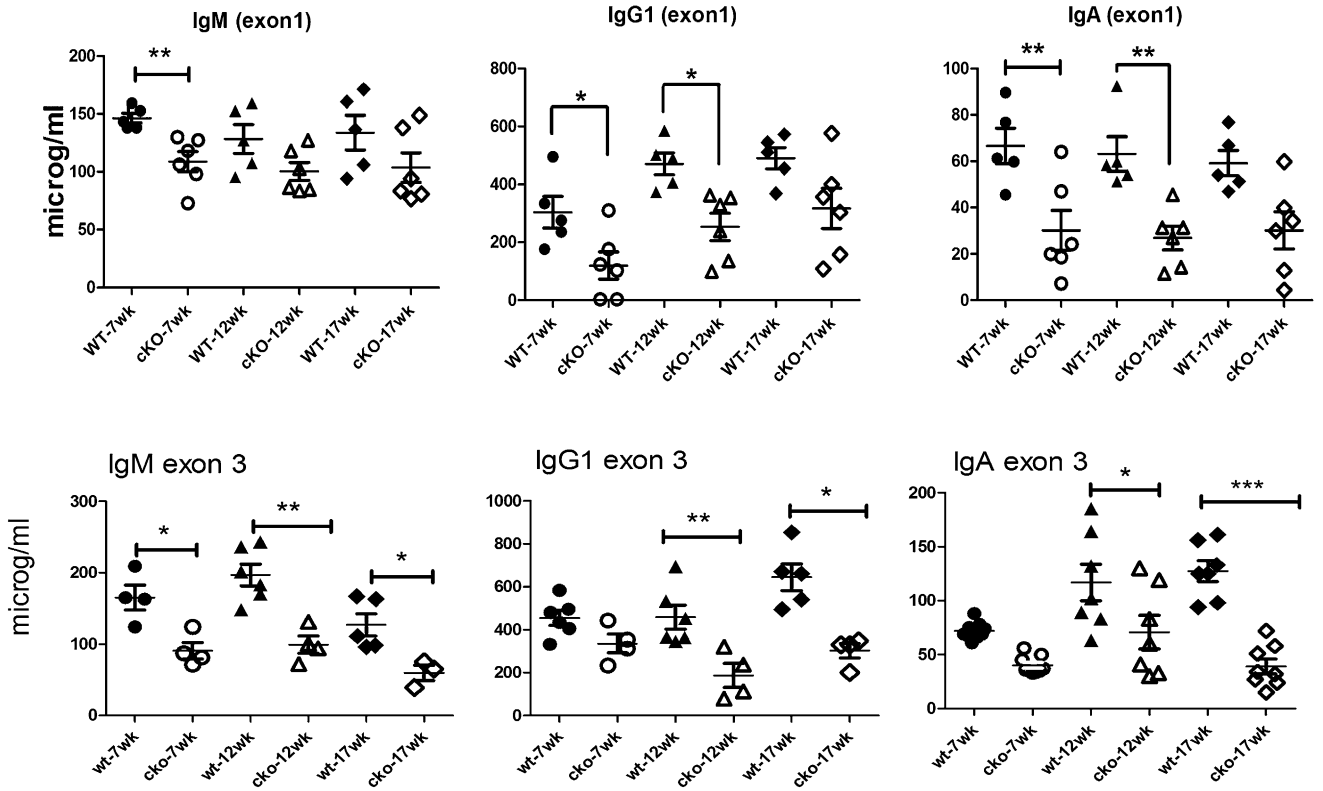

FIGURE 2. Serum levels in naive ELL2$^{loxp/loxp}$ CD19$^{cre/+}$ mice are reduced with both exon 1 and exon 3 deletions. Control mice with either ELL2$^{loxp/loxp}$ CD19$^{+/+}$ or ELL2$^{+/+}$ CD19$^{cre/+}$ (filled symbols, wt) and the ELL2$^{loxp/loxp}$ CD19$^{cre/+}$ mice (open symbols, cKO) were bled at 7, 12, and 17 wk. Serum was analyzed by ELISA for the indicated isotypes. *p = 0.05, **p = 0.01, or ***p = 0.001 as indicated on graphs.

The effect of the cKO of ELL2 is even more evident when the system is challenged by Ag. Mice with a cKO of exon 3 of ELL2 (cKO) between 7 and 8 wk of age were immunized with NP-Ficoll, and serum was drawn at 1, 2, and 3 wk after immunization. ELISAs for NP-specific Abs were conducted. As summarized in Fig. 3, there was significantly less anti-NP Ab of the IgM, IgG2b, and IgG3 isotypes in the exon 3 cKO mice relative to control mice. Next we immunized naive exon 3 ELL2 cKO and control mice with NP-KLH, an Ag that requires T cell help for the B cell responses. As shown in Fig. 3, there was a significantly lower amount of specific anti-NP Ab in the exon 3 NP-KLH–immunized cKO mice of the IgM, IgG1, IgG3, and IgG2c isotypes relative to the control mice. Other isotypes in exon 3–targeted mice were also decreased (data not shown). Thus, we conclude that deletion of ELL2 in stimulated B cells impairs the specific Ab responses to the T-independent Ag, NP-Ficoll, and to the T-dependent Ag, NP-KLH. Upon restimulation with NP-KLH, we observed a recall response in the control mice that was decreased in the cKO mice; data for IgG2c are shown in Fig. 3. Thus, ELL2 is important for Ag-specific responses and immunological memory.

B cell subsets in vivo

The cell-surface markers used for this study are summarized in Supplemental Table I. Analysis by flow cytometry for both the exon 1 and the exon 3 cKO naive mice indicates that there is no significant change in B cell numbers, B1 versus B2 ratios, T cells, or their distribution (data not shown). However, when the ELL2 exon 3–targeted mice were challenged with Ag (NP-Ficoll or NP-KLH), there was a significantly higher percentage of immature and recirculating B cells in the bone marrow after immunization than in the control (Fig. 4). There is a trend to fewer T1 and T2 type B cells in the spleen and a significant decline in T3 cells in the cKOs (Fig. 4B). The Immunological Genome Project (http://immgen.org) profile for ELL2 shows that it is expressed at an intermediate level in these cells. When we determined the number of CD138$^+$ cells, we saw a significant decline in their numbers in the immunized exon 3 ELL2$^{loxp/loxp}$ CD19$^{cre/+}$ mice relative to control mice treated the same way. With the loss of ELL2 in B cells, differentiation can continue to the B220$^+$ IgM$^+$ (new B cell) stage, but the increase in recirculating cells in the bone marrow shown in Fig. 4A indicates a potential problem with further maturation in the spleen, which is evident in the lower numbers of T3 and CD138$^+$ cells produced. We performed ELISPOTS on bone marrow cells from unimmunized exon 1 and exon 3 ELL2 cKO mice using anti-IgG1 Abs. As shown in the results enumerated in Table I, there were significantly fewer IgG1-producing cells in the bone marrow of the cKO mice. These IgG$^+$ cells may represent long-lived PCs or memory B cells (27).

ELL2 deletion influences IgH processing and PC differentiation

After ex vivo LPS stimulation of the naive splenic B cell population in both exon 1 and exon 3 floxed, ELL2 cKOs as compared with CD19$^{+/+}$ controls, we noted a decrease in the production of B220^{lo}CD138$^+$ cells. As shown in a representative experiment in Fig. 5A with an exon 3–deficient mouse, there were ~4-fold fewer cells in the conditional knockout. The cells that had become B220^{lo} CD138$^+$ were sorted and analyzed by PCR to determine whether they were still deleted for exon 3 of ELL2. They were still deficient in ELL2 and do not represent the progeny of a population of undeleted cells (Fig. 5B). The cKO and control cells were equally viable during the course of all the LPS stimulation experiments with both types of cKOs. We isolated RNA from the B220^{lo} CD138$^+$ cells of the two different ELL2 exon knockouts and the control, and subjected the samples to RT-QPCR as described in

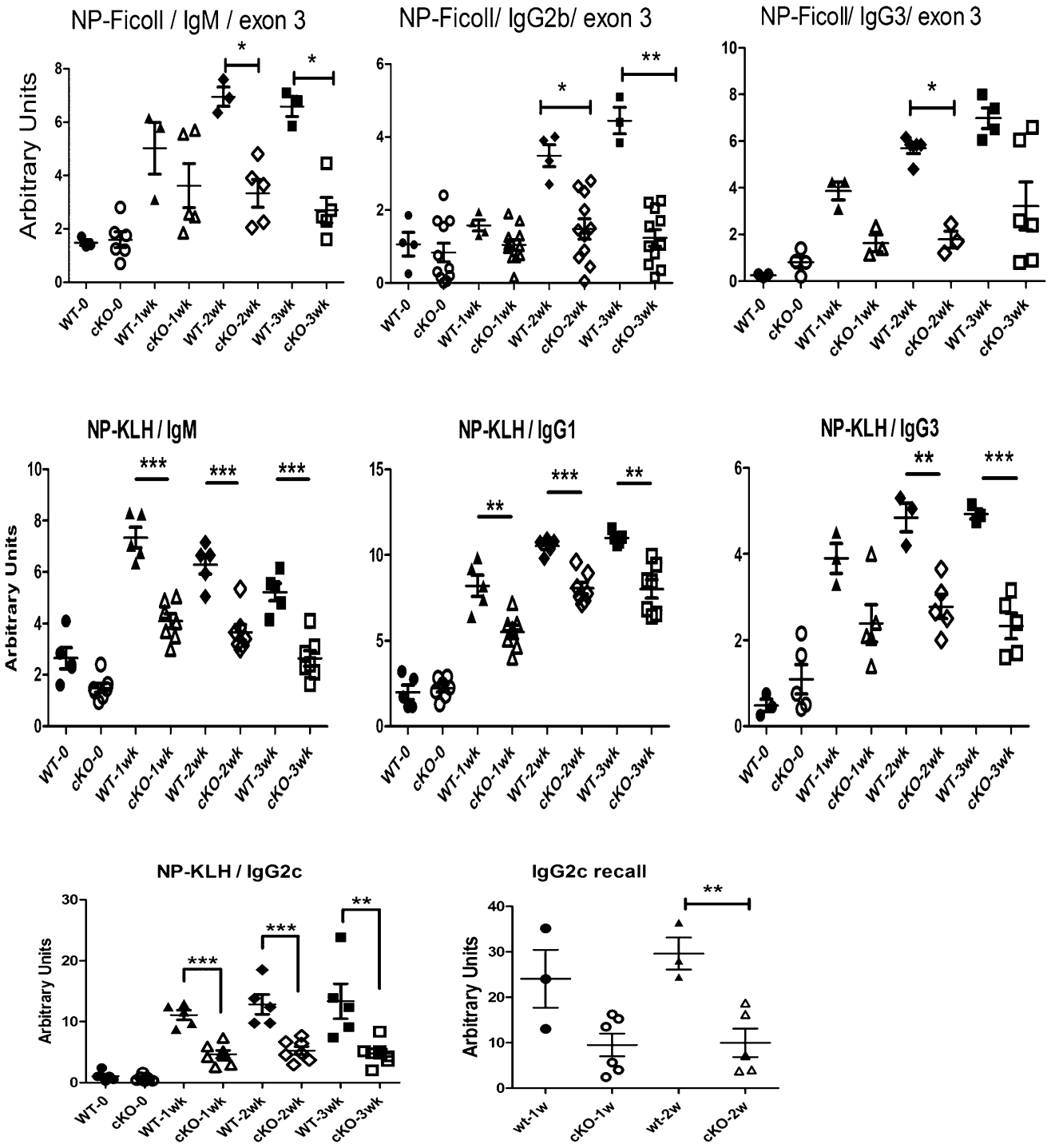

FIGURE 3. NP-Ficoll– and NP-KLH–specific Ab response diminished in immunized ELL2 conditional exon 3 knockout mice. Control mice (filled symbols) and ELL2$^{loxp/loxp}$ CD19$^{cre/+}$ mice (open symbols) were immunized, and serum was drawn at 7, 14, and 21 d after immunization. The amount of NP-specific Ab was determined by ELISA. NP-KLH IgG2c recall response was elicited by immunization 6 wk after the initial dose; serum was collected after 7 and 14 d. *$p = 0.05$, **$p = 0.01$, ***$p = 0.001$.

Materials and Methods. We compared RNA from naive B cells and normalized all the values to HPRT, which had previously been shown to remain constant throughout the B-to-PC transition (28). Production of the secretory-specific IgH μ mRNA is induced dramatically in the control ELL2^{+} cells as expected. In the knockout mice, there was no induction of the secretory-specific H chain mRNA. The overall level of IgH mRNA is reduced in the ELL2 cKO as well; compare the total amount of IgH μ mRNA secretory-specific plus IgH μ mb (Fig. 5D and Tables II, III) in the cKO versus the control. Therefore, ELL2 drives up the amount of mature IgH mRNA, as well as influencing processing. We also saw a decrease in Ig κ mRNA relative to the control (Fig. 5D). Cyclin B2 mRNA was also not as robustly induced in the cKO mice relative to the control B220^{lo}CD138^{+} cells. Examination of XBP1 mRNA revealed a dramatic decrease in both total mRNA and the specifically cytoplasmic spliced form that results from induction of the IRE1 phosphorylation. An ELISPOT to measure IgM secretion, conducted with the B220^{lo}CD138^{+} cells after 4 d of LPS, shows

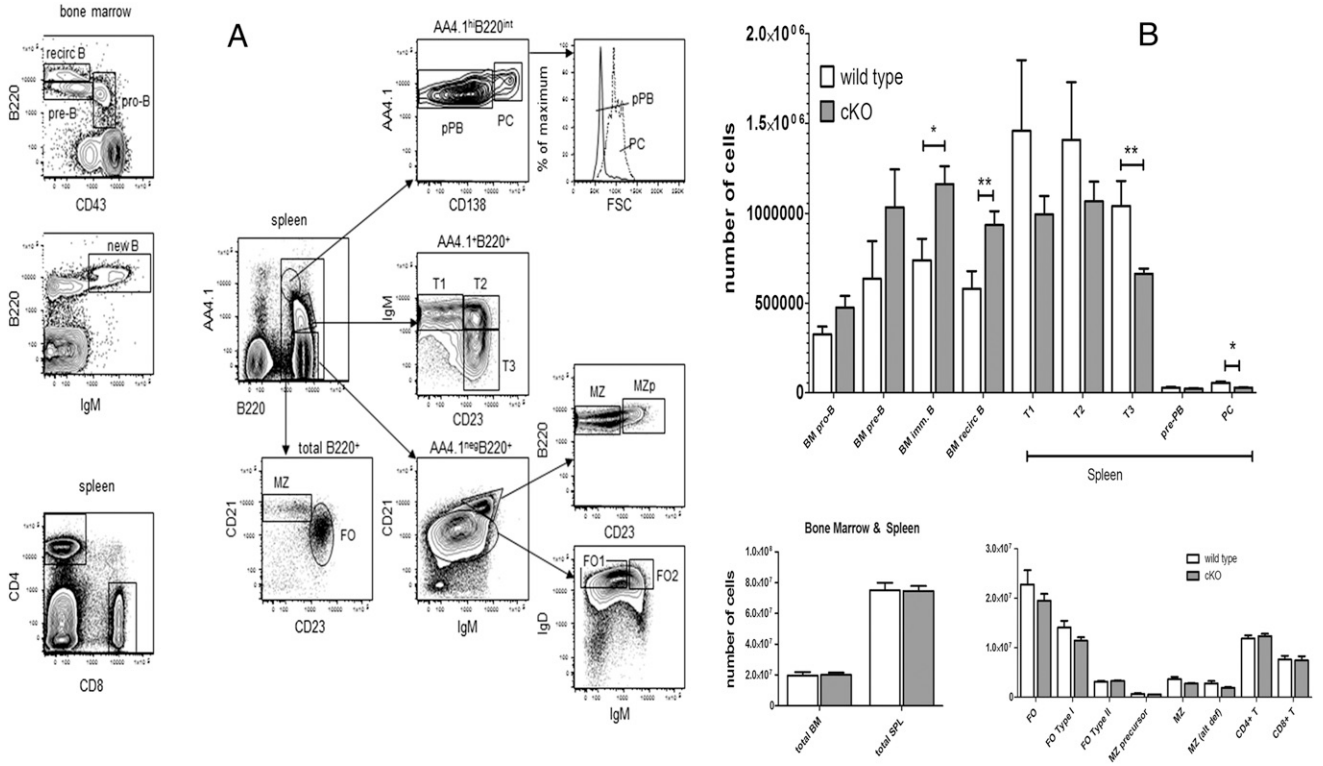

FIGURE 4. ELL2$^{loxp/loxp}$ CD19$^{cre/+}$ mice have increased naive bone marrow cells and decreased T3 and PCs in the spleen. (**A**) Bone marrow and spleen were harvested from mice 21 d after NP-Ficoll or NP-KLH immunization and were subjected to flow cytometry using the indicated Abs. The surface markers used to designate each population are indicated in *Materials and Methods* and Supplemental Table II. (**B**) The number of cells in each of the harvested categories was quantified using the flow data. Error bars are ± SEM. *p = 0.05, **p = 0.01.

a 4.4-fold decreased number of spots, many of which are less intense than those in the control, indicating decreased secretion of IgM in the ELL2 cKO (Fig. 5E and Table I). Thus, as we had predicted based on our previous studies (1), ELL2 is essential for efficient processing to the secretory form of IgH in PCs; in the absence of ELL2, the change-over in RNA processing does not occur, and secreted IgH μ is not induced. In addition, other mRNAs were also reduced in the cKO mice (Table II); these include several in the unfolded response pathway like ATF6, BiP, and OcaB, the transcription of which are thought to be driven by XBP1 (29). BCMA (also known as Tnfrsf17) surface expression is diminished in the ELL2 cKO relative to wild type (wt), as shown in Fig. 5D. Expression of IRF4 and blimp-1 were at or above control levels in the ELL2 cKO B220^{lo}CD138^{+} cells (Table II), so those early steps in B cell activation are largely intact.

The sorted B220^{lo}CD138^{+} cells were fixed and analyzed in the transmission electron microscope (Fig. 6). The cKO cells display an ER that is dilated and fragmented. Similar, distended ER is seen in XBP1 knockout PCs (30). Based on the accumulated data, we conclude that ELL2 deletion has a significant impact on IgH secretory mRNA and protein, XBP1 production, and the activated cell architecture.

Table I. ELISPOT data, splenic B cells, and bone marrow

	Bone Marrow IgG1^{+}		Splenic IgM^{+}, B220^{lo} CD138^{+} Sorted 3-d LPS	
	No. of Spots	Statistics	No. of Spots	Statistics
Control	66	±35 SD	318	±65 SD
cKO ELL2	9	±7 SD	65	±16 SD
p		2.6×10^{-3}		2×10^{-5}

Values normalized to 100,000 cells. The p value is determined by two-tailed t tests. $n \geq 6$ per group.

We then examined the expression of a number of other mRNAs and proteins in the bulk population of control and conditional ELL2 knockout LPS-stimulated cells. We observed normal decreases in the cKO mouse cells in some mRNAs that accompany early steps in PC differentiation; compare plus versus minus LPS values, like ELL3 and C/ebp-β (Table III). Some mRNAs are induced after LPS, both in control and the cKOs like AICDA, PCNA, and Eaf2, a factor associated with the ELL2:pTEFb complex, although their overall levels at the induced state are somewhat less than control. We observed no significant change in the expression of some "housekeeping" genes like Hif1α and Hsp40 in either the controls or the knockouts. A majority of the probes used in the RT-QPCR spanned exons. When we examined the splicing patterns of several of these genes (Bip, Eaf2, IRF4), we saw no difference between control and the ELL2-deficient cells before or after LPS stimulation (data not shown). Thus, some aspects of the PC program are operative. The induction of cyclin B2 mRNA seen in control LPS-stimulated cells was lacking in the cKOs. Cyclin B2 protein resides in the Golgi (31) where carbohydrates are added to secreted proteins; this suggests that the Golgi may also be affected by the lack of a normal UPR.

Changes in mRNA expression were confirmed by analysis of the protein in both exon 1 and exon 3 cKOs. In Fig. 7, protein results from the exon 3 mice are presented. The unconventionally spliced mRNA of XBP1 (XBPs) encodes a protein (32) of ~40 kDa that acts as a transcription factor for upregulation of the UPR genes (33). Because the unconventional XBP1 splicing is initiated by the IRE1α protein after its aggregation and phosphorylation by endo-

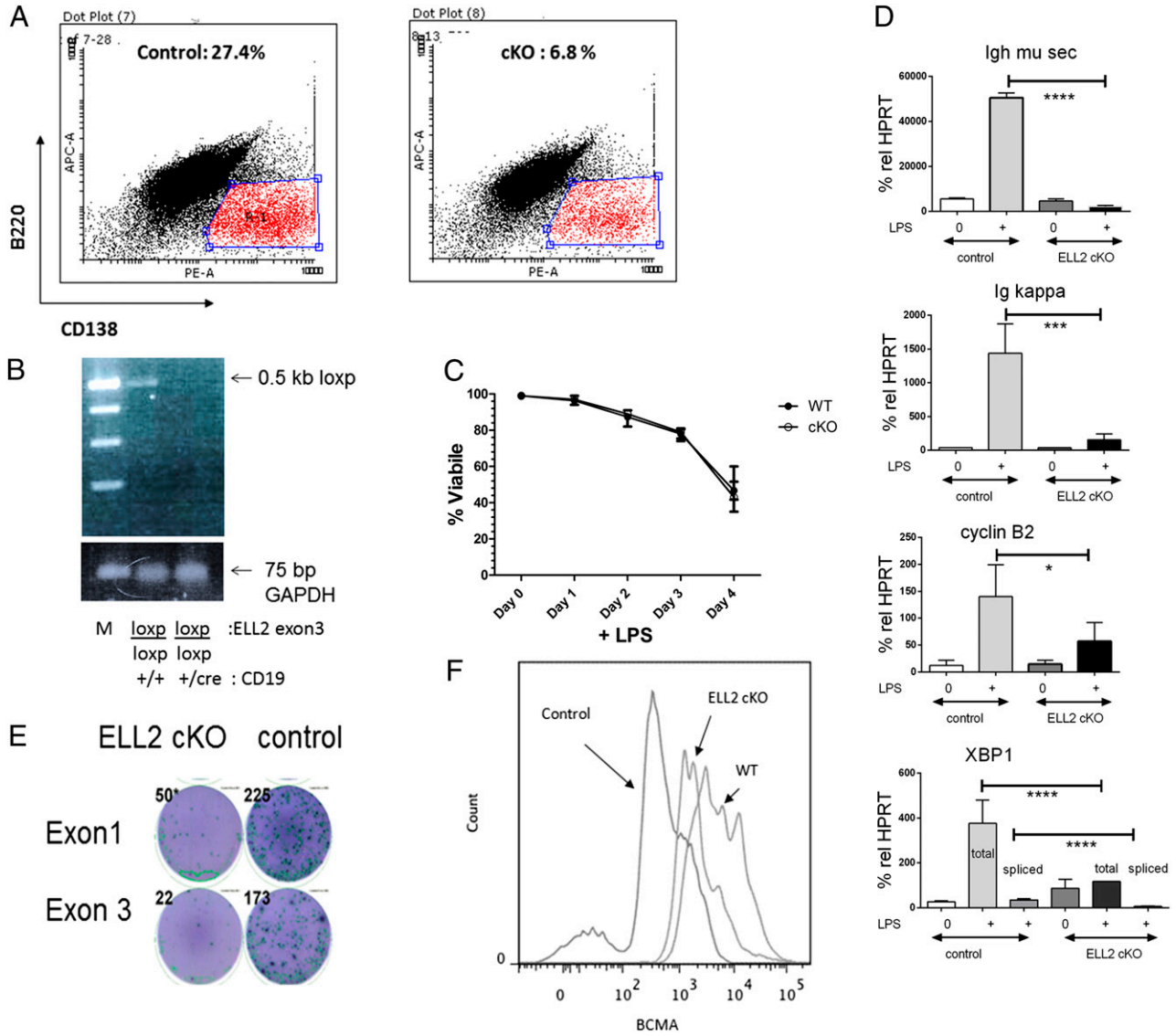

FIGURE 5. ELL2$^{loxp/loxp}$ CD19$^{cre/+}$ influences B220^{lo}CD138^{+} production, IgH secretory mRNA, and XBP1. (**A**) The flow cytometric profile of the LPS-treated splenic B cells from the cKO mice (*left panel*) or the controls (*right panel*). B220^{lo}CD138^{+} cells (boxed) were enumerated as a percentage of the total live cell pool and used for subsequent analyses in (**B**) and (**D**)–(**F**). Splenic B cells were treated with 20 μg/ml LPS for 3 d. (B) PCR of the DNA from the sorted cells, exon $3^{-/-}$ mice shown (see Fig. 1 for details). (**C**) Total cell viability in the LPS culture before sorting was determined by trypan blue staining. (D) RNAs from the sorted B220^{lo}CD138^{+} cells were quantified relative to HPRT using real-time QPCR. Probes specific for the various species are indicated in the Supplemental Table II. Control or ELL2 cKO (ELL2$^{loxp/loxp}$ CD19$^{cre/+}$). Ig μ H chain mRNA secretory-specific mRNA (IgH mu sec; top) was quantified using probes for the 3′ region in the secretory-specific form. The RT-QPCR probes for Ig κ L chain, cyclin B2, and spliced versus unspliced forms of XBP1 mRNA are indicated in the text or Supplemental Table II. Error bars indicate SEM. *p = 0.05, ***p = 0.001, ****p = 0.0001. (E) ELISPOT. Control or cKO mice spleen cells stimulated with LPS for 3 d and sorted for B220^{lo}CD138^{+} (100,000/ well) were assayed for the production of IgM with anti-mouse IgM AP Abs and visualized with NBT/BCIP reagent. Spots were counted in an ELISPOT reader and the data enumerated in Table I. (F) Cells in the B220^{lo}CD138^{+} selected pools were surface stained for BCMA. Control is with no Ab, WT is the ELL2$^{loxp/loxp}$ CD19$^{+/+}$, ELL2 cKO is ELL2 $^{loxp/loxp}$ CD19 $^{cre/+}$.

plasmic reticular stress (34, 35), we investigated the amount and state of IRE1 in our cultures. The level of IRE1α mRNA is only slightly reduced in the conditional ELL2 knockouts relative to the control (Table III). The level of phosphorylated IRE1 protein was determined by Western blotting using anti-pSer724 IRE1 Ab (Fig. 7); increases relative to naive B cells were seen in control and cKOs. These bands were confirmed as IRE1 by reaction with a pan IRE Ab (data not shown). Activation of the novel RNase activity of IRE1 is initiated by dimerization-induced *trans*-autophosphorylation and requires a homodimer of catalytically functional RNase domains (34). When large amounts of protein like secreted Ig or other secretory-associated proteins that may be unfolded are produced, this causes stress to the ER (36). In this study, with reduced levels of BiP, as in the ELL2 cKOs, IRE1 phosphorylation is activated, perhaps in a situation analogous to that of a mutant of IRE1 that cannot bind BiP and remains phosphorylated (37).

Transcription studies

We had previously shown that the alternative processing of the Ig μ H chain is directly regulated by the binding and the action of ELL2 of RNAPII (1). Elongation factors not only change processing patterns, but they also increase the processivity of RNAPII (38), so mRNA yields increase in their presence. We wanted to determine whether ELL2 influences the apparent transcription of some of the other genes we see altered in PC differentiation. We combined ELL2 cDNA with various luciferase reporter constructs

Table II. mRNA expression in $B220^{lo}CD138^{+}$ sorted cells relative to HPRT as 100%

	Control	cKO	Control/cKO
ATF6	**313**	**65**	**4.8**
BiP	1790	536	3.3
Blimp-1	22	25	0.9
ELL1	**52**	**5**	**10.4**
ELL2	**2032**	**<50**	**>37**
ELL3	5	4	1.3
Ire1	272	140	1.9
IRF4	25	32	0.8
Ig μ mb	2138	3093	0.7
OcaB	**2680**	**548**	**4.9**

SEM <5% in all cases, not indicated for clarity; $n > 3$ mice each class, exons 1 and 3. Bolded values show >2-fold change.

bearing promoters in 293 HEK cells and measured luciferase activity (Fig. 8) versus transcription without ELL2. The different promoters showed different levels of luciferase transcriptional induction with ELL2. The cyclin B2 promoter had been cloned into a luciferase reporter by Dr. Engeland, who generous supplied it to us (20). Addition of a cDNA for ELL2 increased luciferase activity from the cyclin B2 promoter almost 12-fold over vector alone, indicating that ELL2 can directly enhance the yield of cyclin B2 promoter–driven mRNA. The positive effect of ELL2 is partially diminished by the addition of p53, which had previously been shown to decrease cyclin B2 transcription (see Supplemental Fig. 2). ELL2 cDNA had no effect on its own promoter, while it stimulated the blimp-1 and IRF4 promoters ~2- to 4-fold. The luciferase construct bearing the 5× UPR element (UPRE) promoter (39), common to many UPR genes (40), was induced >8-fold by ELL2 cDNA, the same induction seen with a cDNA for NF-κB p65 subunit protein (data not shown). Transfections conducted in a B cell line and Jurkat T cells demonstrated a similar pattern of induction with all promoters (data not shown). Thus, ELL2 may participate in the UPR not only by virtue of directing IgH mRNA processing and activating XBP1, but it may also help to increase the levels of the UPR-controlled mRNAs by enhancing their mRNA yields. The ELL2 promoter is stimulated by IRF4 and NF-κB, but not by itself or blimp-1 (Fig. 8). IRF4 binding to the ELL2 promoter by chromatin immunoprecipitation had been shown previously (6). Meanwhile, IRF4 and blimp-1 have transcriptional stimulatory effects on each other. SRp55, implicated in alternative splicing of CD44 and with DNA damage responses (41), significantly enhances blimp transcription (Supplemental Figure 2). SRp55 showed little effect on IgH alternative RNA processing (22). Thus, considering all the evidence presented, we conclude that ELL2 is an essential part of the transcription network leading to PC differentiation; it appears to act between the IRF4/blimp-1 and XBP1 genes.

Discussion

ELL2 floxed conditional deletions, caused by the CD19 promoter–driven cre, decrease basal Ig levels in the serum. In the exon 3 floxed ELL2 cKOs, the responses to immunization with NP-KLH and NP-Ficoll, T-dependent and -independent Ags, respectively, were significantly reduced relative to the controls. In the $CD19^{cre}$-driven deletion of exon 3 floxed ELL2, no gross abnormalities are seen in the number of cells present in the early B cell stages and in total bone marrow and splenic B cells. ELL2 is not maximally expressed until after LPS induction of splenic B cells; then its expression increases as much as 30-fold. This pattern of expression may explain the lack of influence on the early B cell populations because ELL2 is not maximally expressed until after LPS or Ag induction of splenic B cells. In the spleen, deletion of ELL2 in the total B cell population is >90% in the floxed ELL2 alleles, and this percentage persists after LPS stimulation. The large increase in transcription of ELL2 at a point when the CD19 promoter is very active may explain why the gene is so successfully targeted by $CD19^{cre}$.

After ex vivo LPS stimulation of resting B cells, production of secretory-specific IgH μ is significantly reduced in both exon 1 and exon 3 knockouts as judged by mRNA, protein, and ELISPOT

Table III. mRNA expression in wt versus cKO ELL2 mice relative to HPRT set as 100% total in the LPS-stimulated cultures at 3–4 d

Gene	Control No LPS	Control 4-d LPS	cKO no LPS	cKO 4-d LPS	Control/cKO 4-d LPS
AFF1	3	9	0.6	5	1.8
AICDA	0.6	33	1.8	21.3	1.6
ATF6	60	320	64	155	2.1
Bcl6	**1.3**	**5.2**	**1.3**	**2**	**2.6**
BiP	**400**	**1,400**	**432**	**308**	**4.6**
Blimp-1	0.5	48.7	1.0	40.1	1.2
BRD4	100	190	75	80	2.4
Cebp-β	87	43	90	27	1.6
CstF64	1.5	7	2	3	2.3
Cyclin B2	**15**	**65**	**15**	**8**	**8.1**
Eaf1	1.8	6.6	2	4	1.7
Eaf2	7	55	2	35	1.6
ELL3	37	4	50	3	1.3
Hif1a	33	22	25	22	1.0
Hsp40	40	40	38	50	0.8
IgH mb	**3,000**	**2,900**	**2,200**	**6,800**	**0.4**
IgH sec	**5,400**	**45,000**	**2,600**	**1,200**	**37.5**
IRE1	20	270	20	174	1.6
IRF4	1.8	21.2	1.7	21.3	1
NF-κb p50	19	22	22	18	1.2
NF-κb p65	25	18	6	13	1.4
Pax5	36	57	35	45	1.3
PCNA	70	250	150	300	0.8
Sup5H	4	8.5	4	6.5	1.3
XBP1 total	**70**	**405**	**71**	**100**	**4.0**
XBP1 spliced	**4**	**70**	**3**	**3**	**23.3**

SEM <5% in all cases, not indicated for clarity; $n > 6$ mice each class, exons 1 and 3. Bolded values show a greater than 2-fold change.

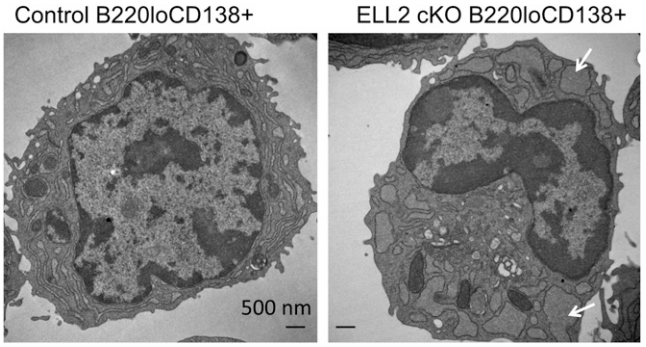

FIGURE 6. Transmission electron microscopy of sorted $B220^{lo}CD138^{+}$ cells (see Fig. 2) from controls (*left*) and the ELL2 cKOs (*right*). Arrows indicate areas of distended ER in the ELL2 cKO cells.

analyses. Production of ex vivo LPS-stimulated, splenic B cells that are $B220^{lo}CD138^{+}$ is reduced by at least 4-fold in the cKOs. Those sorted $B220^{lo}CD138^{+}$ cells lack ELL2 by mRNA and genomic DNA analyses, and have a paucity of secreted IgH and XBP1, with distended, abnormal-appearing ER. In the whole animal, the effect of ELL2 deletion on total Ig production is less profound than that we see in vitro. Our in vitro experiments were done with splenic B2 cells, not B1 cells, and after LPS stimulation; engagement of TLR4 is not the only way to trigger Ig production. Thus, other factors may influence secretory Ig production in B1 cells or in other activation pathways in the whole animal.

IRF4, blimp-1, and XBP1 have been identified as important for PC production (5). When a B cell line ($L29mu^{+}$) was stimulated to convert to the PC phenotype, it did so in a multistep process; proteomic analyses showed that the metabolic capacity and secretory machinery were put into place *before* the mass production of Ig that normally follows (42). Ig secretion in a blimp-1 knockout is low, indirectly through the downstream effects of pax5 suppressing XBP1 (2). When B cells deficient in secretory-specific μ protein ($AID^{-/-}$ $mus^{-/-}$ or $mus^{-/-}$) were stimulated with mitogens, they showed reduced ability to differentiate into $B220^{lo}CD138^{+}$ cells and reduced survival (43). But the absence of secretory Ig protein alone did not prevent XBP1 accumulation, or

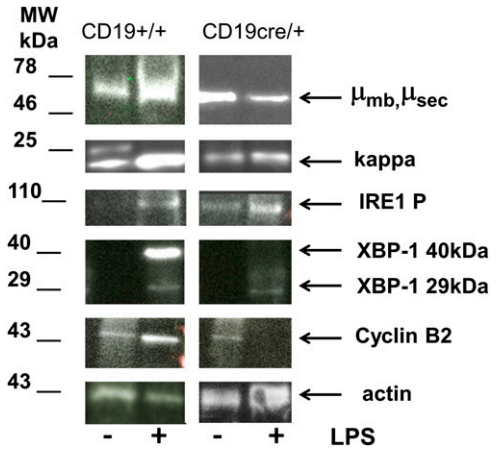

FIGURE 7. Protein expression. Proteins extracted from control ($CD19^{+/+}$ $ELL2^{loxp/loxp}$) and cKO ($CD19^{cre/+}$ $ELL2^{loxp/loxp}$) splenic B cells stimulated for 3 d with LPS (bulk populations) were run on 10% acrylamide SDS-PAGE. Data from an exon 3 deleted mouse shown. The indicated primary and secondary Abs (see *Materials and Methods*) were used in Western blots with ECL substrate. m.w. are extrapolated from kaleidoscope-colored markers run on each gel (data not shown).

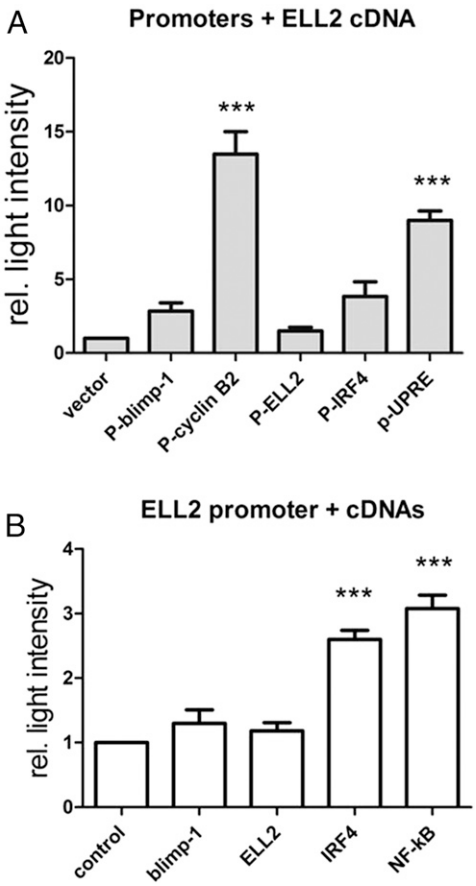

FIGURE 8. ELL2 influences cyclin B2 and UPR expression by stimulating transcription/RNA yields from their promoters. (**A**) The mouse cyclin B2 promoter (−1188 to 0) was cloned into pGL4.10, the luciferase reporter plasmid. 293T cells were cotransfected with the CycB2 reporter, and the indicated cDNA plasmids and luciferase activity measures with a luminometer. (**B**) The ELL2 promoter (−3000 to 0) was cloned into pGL4.11 luciferase reporter and transfected with the indicated cDNA plasmids. ***$p = 0.001$.

XBP1 splicing, which may normally precede upregulation of secreted Ig (33, 43). The hypothesis that the machinery for secretion is put in place before detectable IgH processing to the secreted form was generated. However, what we see in the ELL2 cKOs is that the two processes (establishment of secretory machinery and IgH mRNA processing) appear linked; overall, XBP1 production is reduced along with IgH. It is clear that lack of ELL2 has broader effects than lack of secretory Ig alone, and our luciferase studies show ELL2 can act on cyclin B2 and genes bearing the UPRE to enhance mRNA levels.

Another group used an siRNA-mediated knockdown of ELL2 mRNA in cultured PCs (12). They showed, using deep mRNA sequencing, that the knockdown of ELL2 influenced IgH processing, and expression of several splicing factors, cyclin B2 (ccnb2), and the B cell maturation Ag (tnfrsf17), also known as BCMA. We saw a decrease in IgH secretory mRNA processing, and cyclin B2 and BCMA levels in LPS-stimulated splenic B cells in our knockout mice. Loss of BCMA can contribute to long-term survival (4), and this may be reflected in the reduced number of IgG1 Ab-secreting cells by ELISPOT we saw in bone marrow cells in the knockouts. We saw no major effects on RNA splicing, but rather a significant impairment in the development of the UPRs, perhaps because ELL2 and secreted Ig are important for the establishment of the UPR, but not necessarily for its maintenance, which could be missed by looking only at established PCs.

In the ELL2 knockouts, IRE1α is phosphorylated, but the expression of the downstream proteins for the UPR including spliced XBP1 is reduced in the LPS-stimulated spleens cells. In mature PCs, the ER response is unique from that seen in other cells (44). The UPR in many cells typically has three arms: the IRE-1/XBP pathway, an ATF6 pathway, and the PERK pathway (40). But PERK and ATF6 knockout mice secrete normal amounts of Ig (33, 45). XBP1 conditional deletion mice show defects in PC development (46) and low levels of secretory Ig (47). Thus, when B cells are stimulated, the primary pathway for ER remodeling appears to reside in the IRE1-1 to XBP1 pathway (48). Aggregation and then autophosphorylation of IRE1 cause it to acquire the ability to specifically cleave and then splice XBP1 mRNA; the newly spliced XBP1 RNA species encodes XBP1 protein with transcriptional activity on its own promoter and other UPR promoters containing the UPRE (33, 35). However, the low levels of IgH mRNA in XBP1$^{-/-}$ result from the 8-fold *increased* levels of IRE1P over control; the highly abundant IRE1P cleaves the μ secretory mRNA (49). But a double deletion of XBP1 and IRE1 restores IgM secretion by inhibiting mRNA degradation (49). Taken together, this leads us to a conclusion that Ig secretion can occur without XBP1 cleavage/splicing, and there may be other proteins that allow for the upregulation of the UPR besides the spliced mRNA-encoded XBP1. We believe that ELL2 is one of those proteins; it appears to have a role in enhancing the transcription of other UPR proteins through the UPR element. ELL2 influences more than IgH processing; its effect at enhancing transcription from a variety of promoters, to different extents, implies important specific interactions that remain to be explored.

Acknowledgments

We thank Dr. O.J. Finn and E. Milcarek for encouragement and the Immunology Department, University of Pittsburgh for seed funding for animal model studies.

Disclosures

The authors have no financial conflicts of interest.

References

1. Martincic, K., S. A. Alkan, A. Cheatle, L. Borghesi, and C. Milcarek. 2009. Transcription elongation factor ELL2 directs immunoglobulin secretion in plasma cells by stimulating altered RNA processing. *Nat. Immunol.* 10: 1102–1109.
2. Shaffer, A. L., M. Shapiro-Shelef, N. N. Iwakoshi, A. H. Lee, S. B. Qian, H. Zhao, X. Yu, L. Yang, B. K. Tan, A. Rosenwald, et al. 2004. XBP1, downstream of Blimp-1, expands the secretory apparatus and other organelles, and increases protein synthesis in plasma cell differentiation. *Immunity* 21: 81–93.
3. Ochiai, K., M. Maienschein-Cline, G. Simonetti, J. Chen, R. Rosenthal, R. Brink, A. S. Chong, U. Klein, A. R. Dinner, H. Singh, and R. Sciammas. 2013. Transcriptional regulation of germinal center B and plasma cell fates by dynamical control of IRF4. *Immunity* 38: 918–929.
4. O'Connor, B. P., V. S. Raman, L. D. Erickson, W. J. Cook, L. K. Weaver, C. Ahonen, L.-L. Lin, G. T. Mantchev, R. J. Bram, and R. J. Noelle. 2004. BCMA is essential for the survival of long-lived bone marrow plasma cells. *J. Exp. Med.* 199: 91–98.
5. Nutt, S. L., N. Taubenheim, J. Hasbold, L. M. Corcoran, and P. D. Hodgkin. 2011. The genetic network controlling plasma cell differentiation. *Semin. Immunol.* 23: 341–349.
6. Shaffer, A. L., N. C. T. Emre, L. Lamy, V. N. Ngo, G. Wright, W. Xiao, J. Powell, S. Dave, X. Yu, H. Zhao, et al. 2008. IRF4 addiction in multiple myeloma. *Nature* 454: 226–231.
7. Sciammas, R., A. L. Shaffer, J. H. Schatz, H. Zhao, L. M. Staudt, and H. Singh. 2006. Graded expression of interferon regulatory factor-4 coordinates isotype switching with plasma cell differentiation. *Immunity* 25: 225–236.
8. Shell, S. A., K. Martincic, J. Tran, and C. Milcarek. 2007. Increased phosphorylation of the carboxyl-terminal domain of RNA polymerase II and loading of polyadenylation and cotranscriptional factors contribute to regulation of the ig heavy chain mRNA in plasma cells. *J. Immunol.* 179: 7663–7673.
9. Milcarek, C., M. Albring, C. Langer, and K. S. Park. 2011. The eleven-nineteen lysine-rich leukemia gene (ELL2) influences the histone H3 protein modifications accompanying the shift to secretory immunoglobulin heavy chain mRNA production. *J. Biol. Chem.* 286: 33795–33803.
10. Smith, E., C. Lin, and A. Shilatifard. 2011. The super elongation complex (SEC) and MLL in development and disease. *Genes Dev.* 25: 661–672.
11. Luo, Z., C. Lin, and A. Shilatifard. 2012. The super elongation complex (SEC) family in transcriptional control. *Nat. Rev. Mol. Cell Biol.* 13: 543–547.
12. Benson, M. J., T. Aijö, X. Chang, J. Gagnon, U. J. Pape, V. Anantharaman, L. Aravind, J.-P. Pursiheimo, S. Oberdoerffer, X. S. Liu, et al. 2012. Heterogeneous nuclear ribonucleoprotein L-like (hnRNPLL) and elongation factor, RNA polymerase II, 2 (ELL2) are regulators of mRNA processing in plasma cells. *Proc. Natl. Acad. Sci. USA* 109: 16252–16257.
13. He, N., M. Liu, J. Hsu, Y. Xue, S. Chou, A. Burlingame, N. J. Krogan, T. Alber, and Q. Zhou. 2010. HIV-1 Tat and host AFF4 recruit two transcription elongation factors into a bifunctional complex for coordinated activation of HIV-1 transcription. *Mol. Cell* 38: 428–438.
14. Yang, Q., B. Esplin, and L. Borghesi. 2011. E47 regulates hematopoietic stem cell proliferation and energetics but not myeloid lineage restriction. *Blood* 117: 3529–3538.
15. Borghesi, L., J. Aites, S. Nelson, P. Lefterov, P. James, and R. Gerstein. 2005. E47 is required for V(D)J recombinase activity in common lymphoid progenitors. *J. Exp. Med.* 202: 1669–1677.
16. Santos, P. M., Y. Ding, and L. Borghesi. 2014. Cell-intrinsic in vivo requirement for the E47-p21 pathway in long-term hematopoietic stem cells. *J. Immunol.* 192: 160–168.
17. Winkelmann, R., L. Sandrock, M. Porstner, E. Roth, M. Mathews, E. Hobeika, M. Reth, M. L. Kahn, W. Schuh, and H.-M. Jäck. 2011. B cell homeostasis and plasma cell homing controlled by Krüppel-like factor 2. *Proc. Natl. Acad. Sci. USA* 108: 710–715.
18. Martin, R. M., J. L. Brady, and A. M. Lew. 1998. The need for IgG2c specific antiserum when isotyping antibodies from C57BL/6 and NOD mice. *J. Immunol. Methods* 212: 187–192.
19. Shapiro-Shelef, M., K.-I. Lin, L. J. McHeyzer-Williams, J. Liao, M. G. McHeyzer-Williams, and K. Calame. 2003. Blimp-1 is required for the formation of immunoglobulin secreting plasma cells and pre-plasma memory B cells. *Immunity* 19: 607–620.
20. Krause, K., M. Wasner, W. Reinhard, U. Haugwitz, C. L. Dohna, J. Mössner, and K. Engeland. 2000. The tumour suppressor protein p53 can repress transcription of cyclin B. *Nucleic Acids Res.* 28: 4410–4418.
21. Salsi, V., G. Caretti, M. Wasner, W. Reinhard, U. Haugwitz, K. Engeland, and R. Mantovani. 2003. Interactions between p300 and multiple NF-Y trimers govern cyclin B2 promoter function. *J. Biol. Chem.* 278: 6642–6650.
22. Bruce, S. R., R. W. C. Dingle, and M. L. Peterson. 2003. B-cell and plasma-cell splicing differences: a potential role in regulated immunoglobulin RNA processing. *RNA* 9: 1264–1273.
23. Screaton, G. R., J. F. Cáceres, A. Mayeda, M. V. Bell, M. Plebanski, D. G. Jackson, J. I. Bell, and A. R. Krainer. 1995. Identification and characterization of three members of the human SR family of pre-mRNA splicing factors. *EMBO J.* 14: 4336–4349.
24. Mitani, K., T. Yamagata, C. Iida, H. Oda, K. Maki, M. Ichikawa, T. Asai, H. Honda, M. Kurokawa, and H. Hirai. 2000. Nonredundant roles of the elongation factor MEN in postimplantation development. *Biochem. Biophys. Res. Commun.* 279: 563–567.
25. Rickert, R. C., J. Roes, and K. Rajewsky. 1997. B lymphocyte-specific, Cre-mediated mutagenesis in mice. *Nucleic Acids Res.* 25: 1317–1318.
26. Genovese, C., S. Harrold, and C. Milcarek. 1991. Differential mRNA stabilities affect mRNA levels in mutant mouse myeloma cells. *Somat. Cell Mol. Genet.* 17: 69–81.
27. Zabel, F., D. Mohanan, J. Bessa, A. Link, A. Fettelschoss, P. Saudan, T. M. Kündig, and M. F. Bachmann. 2014. Viral particles drive rapid differentiation of memory B cells into secondary plasma cells producing increased levels of antibodies. *J. Immunol.* 192: 5499–5508.
28. Genovese, C., and C. Milcarek. 1990. Increased half-life of mu Ig mRNA during mouse B-cell development increases abundancy. *Mol. Immunol.* 17: 69–81.
29. Shen, Y., and L. M. Hendershot. 2007. Identification of ERdj3 and OBF-1/BOB-1/OCA-B as direct targets of XBP-1 during plasma cell differentiation. *J. Immunol.* 179: 2969–2978.
30. Taubenheim, N., D. M. Tarlinton, S. Crawford, L. M. Corcoran, P. D. Hodgkin, and S. L. Nutt. 2012. High rate of antibody secretion is not integral to plasma cell differentiation as revealed by XBP-1 deficiency. *J. Immunol.* 189: 3328–3338.
31. Jackman, M., M. Firth, and J. Pines. 1995. Human cyclins B1 and B2 are localized to strikingly different structures: B1 to microtubules, B2 primarily to the Golgi apparatus. *EMBO J.* 14: 1646–1654.
32. Calfon, M., H. Zeng, F. Urano, J. H. Till, S. R. Hubbard, H. P. Harding, S. G. Clark, and D. Ron. 2002. IRE1 couples endoplasmic reticulum load to secretory capacity by processing the XBP-1 mRNA. *Nature* 415: 92–96.
33. Gass, J. N., N. M. Gifford, and J. W. Brewer. 2002. Activation of an unfolded protein response during differentiation of antibody-secreting B cells. *J. Biol. Chem.* 277: 49047–49054.
34. Tirasophon, W., K. Lee, B. Callaghan, A. Welihinda, and R. J. Kaufman. 2000. The endoribonuclease activity of mammalian IRE1 autoregulates its mRNA and is required for the unfolded protein response. *Genes Dev.* 14: 2725–2736.
35. Lee, K., W. Tirasophon, X. Shen, M. Michalak, R. Prywes, T. Okada, H. Yoshida, K. Mori, and R. J. Kaufman. 2002. IRE1-mediated unconventional mRNA splicing and S2P-mediated ATF6 cleavage merge to regulate XBP1 in signaling the unfolded protein response. *Genes Dev.* 16: 452–466.
36. Davenport, E. L., H. E. Moore, A. S. Dunlop, S. Y. Sharp, P. Workman, G. J. Morgan, and F. E. Davies. 2007. Heat shock protein inhibition is associated with activation of the unfolded protein response pathway in myeloma plasma cells. *Blood* 110: 2641–2649.

37. Pincus, D., M. W. Chevalier, T. Aragón, E. van Anken, S. E. Vidal, H. El-Samad, and P. Walter. 2010. BiP binding to the ER-stress sensor Ire1 tunes the homeostatic behavior of the unfolded protein response. *PLoS Biol.* 8: e1000415.
38. Shilatifard, A. 1998. Factors regulating the transcriptional elongation activity of RNA polymerase II. *FASEB J.* 12: 1437–1446.
39. Yoshida, H., T. Okada, K. Haze, H. Yanagi, T. Yura, M. Negishi, and K. Mori. 2000. ATF6 activated by proteolysis binds in the presence of NF-Y (CBF) directly to the cis-acting element responsible for the mammalian unfolded protein response. *Mol. Cell. Biol.* 20: 6755–6767.
40. Takayanagi, S., R. Fukuda, Y. Takeuchi, S. Tsukada, and K. Yoshida. 2013. Gene regulatory network of unfolded protein response genes in endoplasmic reticulum stress. *Cell Stress Chaperones* 18: 11–23.
41. Filippov, V., E. L. Schmidt, M. Filippova, and P. J. Duerksen-Hughes. 2008. Splicing and splice factor SRp55 participate in the response to DNA damage by changing isoform ratios of target genes. *Gene* 420: 34–41.
42. van Anken, E., E. P. Romijn, C. Maggioni, A. Mezghrani, R. Sitia, I. Braakman, and A. J. R. Heck. 2003. Sequential waves of functionally related proteins are expressed when B cells prepare for antibody secretion. *Immunity* 18: 243–253.
43. Kumazaki, K., B. Tirosh, R. Maehr, M. Boes, T. Honjo, and H. L. Ploegh. 2007. AID-/-mus-/- mice are agammaglobulinemic and fail to maintain B220-CD138+ plasma cells. *J. Immunol.* 178: 2192–2203.
44. Ma, Y., Y. Shimizu, M. J. Mann, Y. Jin, and L. M. Hendershot. 2010. Plasma cell differentiation initiates a limited ER stress response by specifically suppressing the PERK-dependent branch of the unfolded protein response. *Cell Stress Chaperones* 15: 281–293.
45. Gass, J. N., H.-Y. Jiang, R. C. Wek, and J. W. Brewer. 2008. The unfolded protein response of B-lymphocytes: PERK-independent development of antibody-secreting cells. *Mol. Immunol.* 45: 1035–1043.
46. Reimold, A. M., N. N. Iwakoshi, J. Manis, P. Vallabhajosyula, E. Szomolanyi-Tsuda, E. M. Gravallese, D. Friend, M. J. Grusby, F. Alt, and L. H. Glimcher. 2001. Plasma cell differentiation requires the transcription factor XBP-1. *Nature* 412: 300–307.
47. Tirosh, B., N. N. Iwakoshi, L. H. Glimcher, and H. L. Ploegh. 2005. XBP-1 specifically promotes IgM synthesis and secretion, but is dispensable for degradation of glycoproteins in primary B cells. *J. Exp. Med.* 202: 505–516.
48. Aragon, I. V., R. A. Barrington, S. Jackowski, K. Mori, and J. W. Brewer. 2012. The specialized unfolded protein response of B lymphocytes: ATF6α-independent development of antibody-secreting B cells. *Mol. Immunol.* 51: 347–355.
49. Benhamron, S., R. Hadar, T. Iwawaky, J.-S. So, A.-H. Lee, and B. Tirosh. 2014. Regulated IRE1-dependent decay participates in curtailing immunoglobulin secretion from plasma cells. *Eur. J. Immunol.* 44: 867–876.